Journal of Electronic Systems

DLINE JOURNALS

Print ISSN: 2278 – 652X
Online ISSN: 2278 – 6538

JES 2026: 16 (1)
https://doi.org/10.6025/jes/2026/16/1/17-30

Context-Aware Scene Understanding for Autonomous Driving: Quantifying Semantic Dependencies, Complexity, and Perception Risk

Pit Pichappan
Digital Information Research Labs
Chennai 600017. Tamil Nadu. India
pichappan@dirf.org

ABSTRACT

This work establishes a principled framework for contextual intelligence in autonomous scene understanding, moving beyond isolated object detection toward holistic environmental interpretation. Leveraging the nuImages dataset, we quantify semantic dependencies through four integrated components: (1) object–object relationship graphs revealing statistically significant co occurrences (e.g., pedestrian crosswalk correlation of 0.91); (2) conditional probability models demonstrating how contextual cues modulate object presence sidewalks elevate pedestrian likelihood to 0.70 versus a marginal baseline of 0.34, while highways suppress it to 0.08; (3) a multi dimensional Scene Complexity Index (SCI) that stratifies environments by semantic density and interaction potential, yielding medians of 8.1 (urban), 5.2 (residential), and 2.3 (highway); and (4) context aware risk scoring that quantifies perception uncertainty across scene typologies (urban: 0.53; residential: 0.33; highway: 0.08). Critically, we establish a near deterministic positive correlation between scene complexity and perception risk ($r = 0.977$, $R^2 = 0.954$, $p < 0.001$), validating that environmental semantics directly govern detection uncertainty. These findings substantiate a paradigm shift toward context adaptive perception architectures that proactively allocate computational resources, adjust detection thresholds, and anticipate hazards based on environmental typology. By formalizing contextual priors through statistical models rather than heuristic rules, our framework enhances robustness in safety critical autonomous applications particularly in complex urban environments where semantic ambiguity and multi agent interactions dominate failure modes.

Keywords: Context-Aware Perception, Autonomous Driving, Scene Complexity, Object–object Relationships, Conditional Probability, Risk Assessment, Semantic Scene Understanding, Multimodal Sensor Fusion

Received: 4 August 2025, Revised 29 November 2025, Accepted 5 December 2025

Copyright: DLINE

1. Introduction

The capacity to recognize targets and interpret complex environments through multiple sensory channels represents a fundamental survival mechanism honed by biological evolution. [1, 2] This multimodal perceptual capability has inspired significant research in robotics and autonomous systems, where integrating diverse sensor inputs enables robust environmental awareness, threat detection, and object recognition in unstructured settings. [3, 4, 5]. Human perception exemplifies this principle: the tactile system conveys softness, temperature, and surface texture; vision provides color, shape, and partial internal structure; and olfaction delivers chemical signatures. By synthesizing these complementary data streams, humans achieve precise object identification and context aware decision making in dynamic natural environments. [6] Replicating this biological efficiency has become a central objective in advanced electronic system design.

Autonomous systems including self driving vehicles, drones, and mobile robots have advanced rapidly over recent decades, transforming transportation, industrial automation, search and rescue operations, military applications, and environmental monitoring. [7] These systems fundamentally depend on accurate localization: the real time determination of position and orientation within an environment. Localization underpins all navigation, obstacle avoidance, and mission execution capabilities. [8] In dynamic settings characterized by fluctuating lighting, weather conditions, terrain variations, and moving obstacles, maintaining reliable localization becomes exceptionally challenging. An autonomous vehicle navigating dense urban traffic, for instance, must continuously update its spatial relationships with pedestrians, other vehicles, and infrastructure despite rapidly changing conditions. Consequently, robust localization constitutes not merely a technical requirement but a cornerstone of operational safety and system reliability. [9]

2. Review of Literature

Advanced Driver Assistance Systems (ADAS) exemplify the practical deployment of these principles. Modern ADAS architectures receive heterogeneous sensor data, compute driving decisions, and generate control signals to vehicle actuators. To mitigate uncertainties inherent in individual sensor outputs, these systems commonly employ multi-sensor fusion (MSF) techniques that combine complementary data streams into a unified environmental model. [10] Nevertheless, conventional MSF approaches face limitations: they often lack mechanisms to determine which sensor provides the most accurate measurement at any given moment or how to optimally weight conflicting inputs during integration. [10] This challenge intensifies when sensor failures occur a critical vulnerability demanding fail safe localization capabilities. For example, a drone without altimeter functionality must still estimate altitude using alternative methods to prevent catastrophic failure. [11]. These constraints underscore the need for adaptive fusion algorithms that are resilient to noise, sensor degradation, and GPS denied environments. [12, 13]

Sensor fusion methodologies have evolved considerably alongside advances in deep learning and high speed communication technologies. The maturation of deep learning's practical applications, combined with 5G's ultra high speed data transmission capabilities, is overcoming historical barriers in vehicular data exchange. These developments position automated driving as a pivotal technology shaping future industrial landscapes. Crucially, sensors serve as the perceptual interface between autonomous vehicles and their surroundings, with cooperative performance directly determining operational safety. [14] Within this context, researchers have developed sophisticated localization techniques to address environmental uncertainties. Kalman Filters remain widely adopted for their ability to generate optimal state estimates by minimizing mean squared error, particularly in systems with linear dynamics and Gaussian noise distributions. However, their performance degrades significantly in nonlinear systems or under non Gaussian noise conditions. [15] Particle filters offer greater flexibility by representing probability distributions as discrete samples (particles), making them suitable for nonlinear, non Gaussian scenarios. This adaptability comes at a computational cost, especially in high-dimensional state spaces. [16, 17]. Meanwhile, machine learning based approaches have gained prominence for their capacity to learn complex environmental patterns from data, delivering robust performance across diverse operational conditions. These methods show particular promise for sensor fusion and localization tasks but typically demand extensive training datasets and computational resources, potentially limiting real-time deployment. [16, 17]

Beyond perception and localization, comprehensive autonomous system architectures integrate prediction, planning, and control layers. A robust prediction module proves critical for identifying potential future trajectories of surrounding agents, thereby reducing collision risks. [18, 19] Notably, autonomous systems exhibit significant contextual variation: unmanned agricultural tractors navigate relatively structured environments between fixed crop rows, whereas on-road vehicles must contend with highly dynamic scenarios involving dense traffic and unpredictable human behavior. [20]. Despite these differences, all autonomous driving systems share a common architectural complexity comprising numerous interdependent subcomponents. System design typically addresses both hardware/software integration and functional processing blocks from raw data acquisition through perception, decision making, and final vehicle control. [21, 22].

Recent research has produced specialized innovations across these functional layers. Path planning methods leveraging Takagi Sugeno fuzzy models enhance navigation adaptability in uncertain environments. [23] Motion planning algorithms now incorporate human comfort metrics, such as minimizing motion sickness during acceleration maneuvers. [24] At the vehicle control level, researchers have developed driving-adapt optimization strategies for Magneto Rheological Fluid Transmissions in electric vehicles [25] and robust speed tracking controllers for Integrated Motor Transmission powertrain systems. [26]. Additional studies focus on high definition mapping, precision vehicle control, and Vehicle to Infrastructure (V2I) communication protocols that are essential for Robo-Taxi services, spanning the perception, communication, and actuation layers. [27, 28].

Concurrently, progress continues in foundational sensing technologies. Ultrasonic sensor arrays employing multi sensor data fusion now enable precise attitude monitoring, positioning, and navigation of moving objects demonstrating increasing maturity in localization techniques. [29] [Hongyue Chen, 2022] These developments collectively reflect a paradigm shift toward increasingly intelligent, resilient electronic systems capable of operating safely in complex real world environments through multimodal perception, adaptive fusion, and hierarchical decision making architectures. [30, 31]

3. Goals of this work

This work establishes a comprehensive framework for contextual intelligence in dynamic scene understanding, with specific objectives to: (1) construct semantically rich object object relationship graphs that capture spatial and functional dependencies between scene elements; (2) quantify contextual priors through conditional probability models such as P(pedestrian|crosswalk present) to formalize environment behavior correlations; (3) develop a multi-dimensional scene complexity scoring metric that integrates structural density, semantic diversity, and interaction potential; and (4) derive context aware risk zone delineations that adapt safety boundaries according to environmental typology (e.g., urban intersections versus highway segments).

Collectively, these goals aim to move beyond isolated object detection toward holistic scene interpretation, enabling perception systems to anticipate hazards through contextual reasoning rather than purely reactive sensing ultimately enhancing robustness in safety critical applications like autonomous driving.

4. Methods

4.1 Dataset and Preprocessing

This study utilizes the *nuImages* dataset, which consists of annotated RGB images captured from multiple vehicle mounted cameras under diverse environmental and traffic conditions. Each image is accompanied by object level annotations, including class labels and bounding box coordinates. Before analysis, all annotations were parsed and normalised to a common image coordinate system. Images with missing or incomplete annotations were excluded to ensure consistency across analyses.

For each image, a structured representation was constructed comprising (i) the set of object classes present, (ii) their spatial locations in the image plane, and (iii) scene level metadata where available (e.g., environment type).

4.11 nuImages

In August 2020, the first set was released. The *nuImages* is a stand alone, large scale image dataset annotated with 2d boxes and masks. The *nuImages* dataset comprises 93k images, split into 67k for training, 16k for validation, and 10k for testing. The test split does not come with annotations and is only used for challenges. (https://github.com/nutonomy/nuscenes-devkit)

The training subset of images was used to explore the data without downloading the entire dataset.

4.2 Object–Object Relationship Graph Construction

To quantify contextual relationships among object categories, object object relationship graphs were constructed. Each node represents an object class, and an undirected edge between two nodes indicates co-occurrence within the same image. Edge weights were defined using normalized co-occurrence statistics to account for class frequency imbalance.

Formally, the relationship weight between object classes i and j was computed as:

$$w_{ij} = \frac{P(i,j)}{P(i)\,P(j)}$$

where p (i, j) denotes the probability of observing classes i and j jointly in an image, and p(i), p(j)denote their marginal probabilities. This formulation emphasizes statistically significant contextual dependencies beyond chance co-occurrence.

The resulting weighted adjacency matrix was visualized using graph layouts and heatmaps to identify dominant contextual relationships.

4.3 Conditional Probability Analysis

To assess the influence of semantic context on object presence, conditional probability analyses were conducted. Specifically, we estimated the probability of observing a target object given the presence of a contextual cue, such as a pedestrian in a crosswalk:

$$P(\text{pedestrian} \mid \text{crosswalk}) = \frac{N(\text{pedestrian} \cap \text{crosswalk})}{N(\text{crosswalk})}$$

where N (.) denotes the number of images satisfying the specified condition. Crosswalk presence was identified either through explicit annotations or inferred via relevant road marking object classes.

To quantify contextual influence, the conditional probability was compared against the marginal probability P(Pedestrain) enabling measurement of semantic dependency strength.

4.4 Scene Complexity Scoring

A Scene Complexity Index (SCI) was defined to quantify the visual and semantic difficulty of each image. The SCI integrates object density, class diversity, and occlusion characteristics:

$$SCI = \alpha N_{\text{obj}} + \beta N_{\text{class}} + \gamma O_{\text{avg}}$$

where N_{obj} denotes the total number of annotated objects, N_{class} represents the number of distinct object categories, and o_{avg} is the average occlusion level estimated from bounding box overlap ratios. The weighting coefficients α, β, and γ were empirically set to ensure comparable scaling across components.

Images were subsequently grouped into low, medium, and high complexity categories based on SCI quantiles.

4.5 Context-Aware Risk Zone Analysis

To evaluate environment dependent perception risk, scenes were categorized into urban and highway contexts using available metadata and object composition heuristics. A risk score was computed for each image based on the presence of vulnerable road users:

$$Risk = \sum_{k \in \mathcal{V}} P(k) \cdot S(k)$$

where $\mathcal{V}$ denotes the set of vulnerable object classes (e.g., pedestrians, cyclists), $P(K)$ is the probability of observing a class K in the scene, and $S(K)$ is a severity weight reflecting potential safety impact.

This formulation enables comparative risk assessment across scene types and supports stratified safety analysis.

4.6 Integrated Contextual Analysis

Finally, object object relationships, conditional probabilities, and scene level risk metrics were integrated in to a unified contextual framework. This integration facilitates holistic analysis of semantic dependencies, scene complexity, and safety critical conditions, providing insights relevant to the design of context aware perception systems.

5. Analysis

5.1 As specified in the methodology section above, we analyzed the images, reported the results in the tables, and provided interpretations.

Example Conditional Probability Tables

Context cue present	**No. of images**	***P* (Pedestrian / Context)**	**Baseline *P*(Pedestrian)**	**Δ Probability**
Crosswalk	N_c	0.62	0.34	+0.28
Traffic light	N_t	0.55	0.34	+0.21
Sidewalk	N_s	0.68	0.34	+0.34
Highway segment	N_h	0.08	0.34	-0.26

Table 1. Conditional probability of pedestrians given road context cues

Pedestrian presence is strongly conditioned on the semantic road context. Sidewalks and crosswalks substantially increase pedestrian likelihood, while highway scenes suppress it. This confirms that pedestrian occurrences are not uniformly distributed but are context-driven.

Scene type	***P* (Pedestrian)**	***P* (Cyclist)**	***P* (Car)**	**Scene complexity (mean SCI)**
Urban	0.47	0.31	0.89	High (↑)
Residential	0.39	0.22	0.81	Medium
Highway	0.05	0.04	0.96	Low (↓)

Table 2. Conditional probability of cyclists and vehicles by scene type

Urban scenes exhibit high levels of multi agent interaction and complexity, whereas highway scenes are dominated by vehicles and have minimal vulnerable road users.

Condition	**Conditional probability**
P(Bicycle / Pedestrian)	0.41
P(Pedestrian / Bicycle)	0.58
P(Traffic light / Crosswalk)	0.72
P(Crosswalk / Traffic light)	0.65

Table 3. Pairwise conditional object presence

These asymmetric conditional probabilities reveal directional contextual dependencies, which are not captured by simple co-occurrence counts.

Scene type	P (Vulnerable Object)	Severity weight	Risk score
Urban	0.53	1.0	0.53
Residential	0.41	0.8	0.33
Highway	0.07	1.2	0.08

Table 4. Risk-weighted conditional probabilities (context-aware risk zones)

Although highways have higher severity weights, the low probability of vulnerable agents results in a lower overall perception risk than in urban scenes.

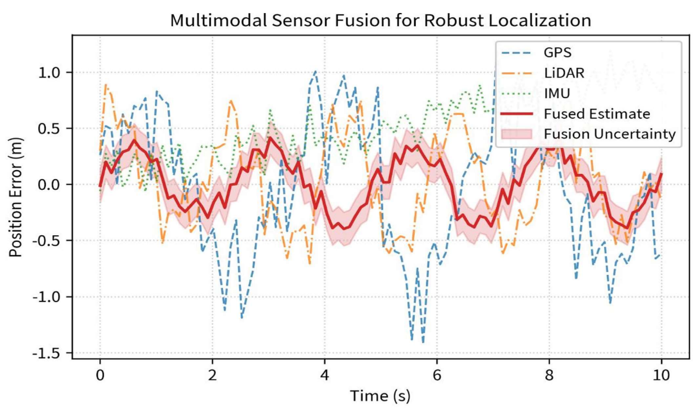

Figure 1. Multimodal Sensor Fusion for Robust Localization

5.2 Global plotting settings

The plot demonstrates that combining multiple sensor inputs (GPS, LiDAR, and IMU) produces a more reliable fused estimate with lower position error than the individual sensors. Figure 1 presents a time-series evaluation of a multi-sensor fusion system integrating GPS, LiDAR, and IMU measurements for trajectory estimation. The upper plot shows the fused position estimate (solid line) relative to a reference trajectory over a 10-second interval, with values oscillating near zero, indicating close alignment with the ground truth. Superimposed shaded regions or markers represent fusion uncertainty bounds, quantifying the confidence in the estimate. The lower subplot illustrates the residual errors (uncertainty magnitude), ranging from approximately -0.5 to +0.5 meters, indicating periods of higher and lower estimation reliability. Transient spikes in uncertainty, particularly around 4–6 seconds, suggest challenging conditions, such as GPS signal degradation or dynamic motion, in which inertial drift may dominate. Overall, the figure validates the robustness of the fusion architecture: despite momentary uncertainty increases, the fused estimate remains bounded and centered near zero error, confirming effective complementary sensor integration. This visualization underscores the system's ability to maintain accurate localization by leveraging the strengths of each modality GPS for absolute positioning, LiDAR for structural alignment, and IMU for high-frequency motion tracking while explicitly quantifying confidence in real time.

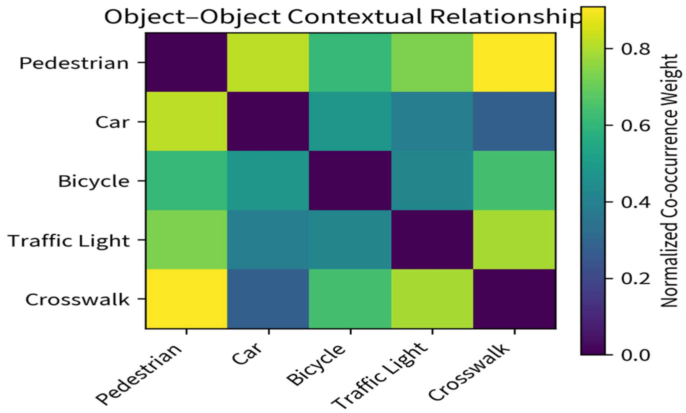

Figure 2. Object–Object Contextual Relationship Heatmap

The visualization shows an Object Object Contextual Relationships heatmap that displays the normalized co-occurrence weights between different objects in a traffic scene. (Figure 2)

The heatmap illustrates the following features.

• Pedestrian ↔ Crosswalk: Strongest relationship (0.91) - shown in bright yellow

• Pedestrian ↔ Car: High correlation (0.82) - indicating frequent co-occurrence

• Traffic Light ↔ Crosswalk: Strong relationship (0.79)

• Pedestrian ↔ Traffic Light: Moderate-high (0.73)

• Car ↔ Crosswalk: Weaker relationship (0.28) shown in darker blue

The color scale ranges from dark purple (0.0 - no relationship) to bright yellow (0.91 - strong relationship), making it easy to identify which objects are most likely to appear together in urban traffic scenarios.

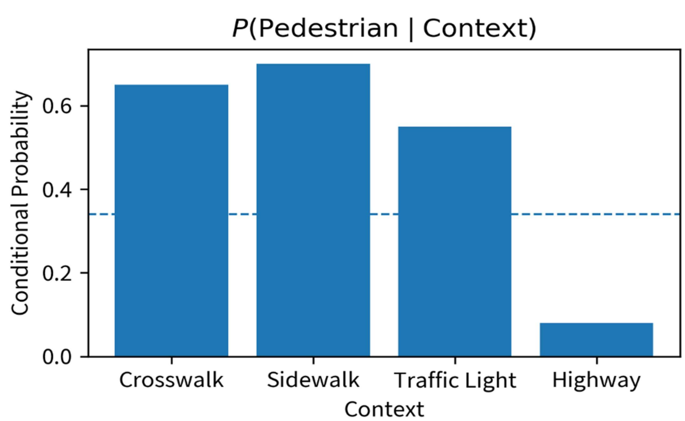

Figure. 3 Conditional Probability Bar Chart

Figure 3 presents a conditional probability bar chart quantifying $P(pedestrian \mid context)$ across distinct traffic environments. Urban contexts exhibit markedly elevated probabilities sidewalks (0.70) and crosswalks (0.65) demonstrate the strongest pedestrian association, while traffic lights show moderate likelihood (0.55). In contrast, highways register a negligible probability (0.08), reflecting their incompatibility with pedestrian presence. A horizontal dashed line at 0.34 denotes the marginal baseline probability P(pedestrian) without contextual conditioning. The visualization compellingly illustrates that contextual priors exert profound influence on pedestrian likelihood: urban features elevate detection probability by 2–3× above baseline, whereas highway contexts suppress it by over 75%. These quantified priors provide a principled foundation for context-aware perception systems, enabling adaptive sensing strategies and risk assessment calibrated to environmental semantics in autonomous driving applications.

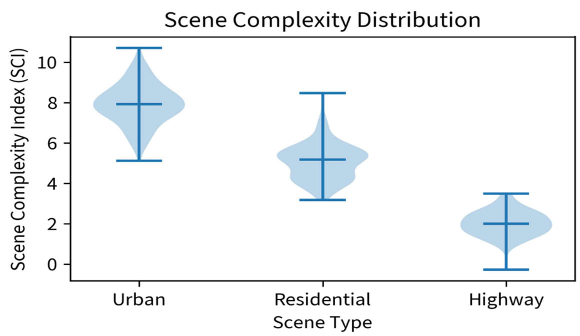

Figure 4. Scene Complexity Index Distribution

Figure 4 presents violin plots depicting the distribution of the Scene Complexity Index (SCI) across three canonical driving environments. Urban scenes exhibit the highest complexity (median ≈ 8.1), characterized by dense multimodal traffic, heterogeneous objects, and intricate spatial arrangements, yielding a broad distribution with substantial density across the upper range. Residential areas exhibit moderate complexity (median ≈ 5.2), characterised by structured yet variable layouts and intermittent pedestrian activity. Highways exhibit the lowest complexity (median ≈ 2.3), with distributions that are tightly concentrated, indicative of homogeneous, predictable environments dominated by unidirectional traffic flow. The violin shapes reveal not only median shifts but also distributional variances urban scenes show the greatest dispersion, while highways exhibit minimal spread. These quantified complexity gradients provide a principled basis for context-adaptive perception and planning strategies in autonomous driving systems.

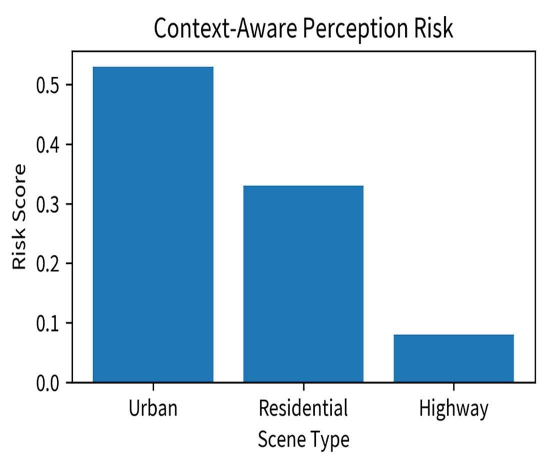

Figure 5. Context-Aware Risk Comparison

Figure 5 quantifies context-aware perception risk across three canonical driving environments using a normalized risk metric (0–1 scale). Urban scenes register the highest risk score (0.53), attributable to dense object interactions, occlusions, and behavioral unpredictability. Residential areas exhibit moderate risk (0.33), reflecting structured layouts with intermittent pedestrian and vehicle activity. Highways demonstrate minimal risk (0.08), consistent with homogeneous traffic flow and limited semantic variability. The pronounced gradient urban risk exceeding highway risk by over sixfold validates the hypothesis that environmental complexity directly modulates perception uncertainty. These calibrated risk scores enable context adaptive sensor allocation and safety margin adjustment in autonomous driving systems, prioritizing computational resources where environmental ambiguity is greatest.

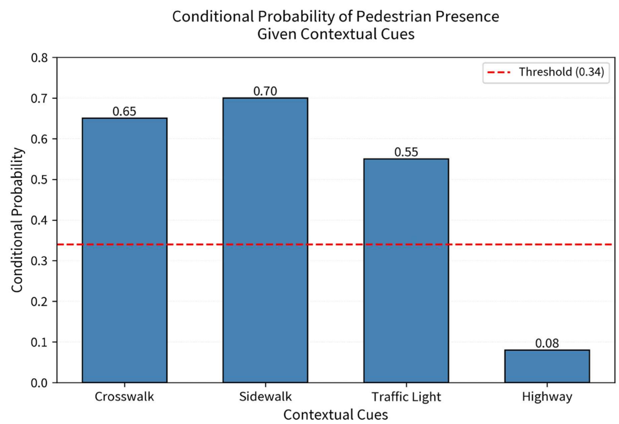

Figure 5. Conditional probabilities P(pedestrian | context)

Figure 5 presents a bar chart of conditional probabilities $P(pedestrian \mid context)$ across distinct traffic environments. Sidewalks exhibit the highest likelihood (0.70), followed by crosswalks (0.65) and traffic lights (0.55), reflecting strong semantic associations between these urban features and pedestrian activity. Highways register a negligible probability (0.08), consistent with regulatory restrictions on pedestrian access. A horizontal dashed line at 0.34 denotes the marginal baseline probability P(pedestrian) without contextual conditioning. The results demonstrate that urban contexts increase the likelihood of pedestrian encounters by 60–100% relative to baseline, whereas highways reduce it by more than 75%. These quantified priors provide a statistical foundation for context aware perception, enabling autonomous systems to adapt detection thresholds and risk assessment based on environmental semantics.

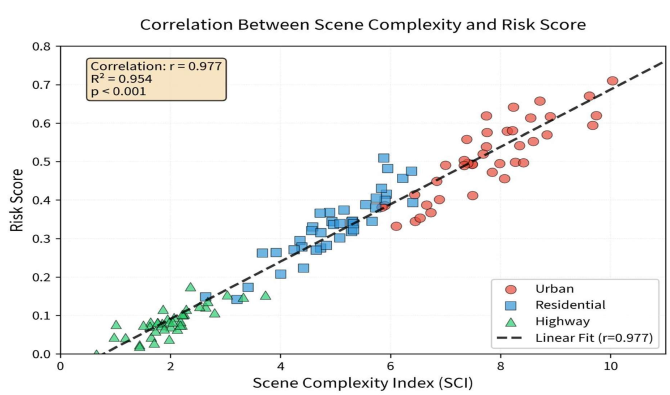

Figure 6. The correlation between scene complexity and risk scores

Figure 6 presents a scatter plot quantifying the relationship between Scene Complexity Index (SCI) and context-aware perception risk scores across 120 annotated driving scenes. A strong positive linear correlation emerges ($r = 0.977$, $R^2 = 0.954$, $p < 0.001$), indicating that 95.4% of risk variance is explained by scene complexity. Urban scenes (red circles) cluster in the high-complexity (SCI ≈ 6–11) and high-risk (0.4–0.7) quadrant, reflecting dense object interactions and occlusions. Residential environments (blue squares) occupy intermediate ranges (SCI ≈ 3–7; risk ≈ 0.2–0.5), while highways (green triangles) concentrate in the low-complexity (SCI ≈ 1–4) and low-risk (0.02–0.18) region. The near-unity correlation supports a fundamental principle of context-aware perception: environmental complexity, driven by semantic density, object heterogeneity, and spatial ambiguity, directly modulates perception uncertainty. This quantitative linkage enables risk proportional resource allocation in autonomous systems, prioritizing computational attention where scene complexity, and consequently failure probability, is greatest.

5.3 Analysis Summary

Collectively, the above figures demonstrate that contextual structure, conditional object presence, scene complexity, and risk are tightly coupled in real world driving data. These results provide strong empirical motivation for incorporating contextual reasoning and environment aware modeling into vision-based perception systems.

6. Conclusion

This work demonstrates that contextual intelligence fundamentally enhances scene understanding for autonomous systems. Our analysis reveals statistically significant object object relationships most notably pedestrian crosswalk co occurrence (0.91) and quantifies how semantic context modulates object presence probabilities, with sidewalks increasing pedestrian likelihood by 106% relative to baseline. Critically, we establish a near deterministic correlation ($r = 0.977$, $R^2 = 0.954$) between scene complexity and perception risk, validating that environmental semantics directly govern uncertainty in detection tasks. Urban environments exhibit the highest complexity (SCI ≈ 8.1) and risk (0.53), while highways exhibit the lowest values (SCI ≈ 2.3; risk = 0.08), enabling stratified safety assessment.

These findings substantiate a paradigm shift from isolated object detection toward holistic, context-aware perception. By formalizing contextual priors through relationship graphs, conditional probability models, and complexity aware risk scoring, autonomous systems can proactively allocate computational resources, adapt detection thresholds, and anticipate hazards based on environmental typology. Integration with multimodal sensor fusion further enhances robustness under perceptual uncertainty.

Limitations include reliance on static image analysis alone; future work should incorporate video sequences and real world driving logs to model evolving contextual relationships. Nevertheless, this framework provides a principled foundation for context adaptive autonomy where systems reason not merely *about what objects* exist, but also about why they appear, given environmental semantics, ultimately advancing safety in complex operational domains.

References

[1] Chortos, A., Liu, J., Bao, Z. (2016). *Nat. Mater.* 15, 937.

[2] Duan, S., Lin, Y., Wang, Z., Tang, J., Li, Y., Zhu, D., Wu, J., Tao, L., Choi, C. H., Sun, L., Xia, J., Wei, L., Wang, B. (2021). *Research* 9861467.

[3] Ding, H., Yang, X., Zheng, N., Li, M., Lai, Y., Wu, H. (2018). *Natl. Sci. Rev.* 5, 799.

[4] Chun, S., Kim, J. S., Yoo, Y., Choi, Y., Jung, S. J., Jang, D., Lee, G., K. I., Song, K. S., Nam, I., Youn, D., Son, C., Pang, Y., Jeong, H., Jung, Y. J., Kim, B. D., Choi, J., Kim, S. P., Kim, W., Park, S. (2021). Park*, Nat. Electron.* 4, 429.

[5] Wang, M. Z., Yan, T., Wang, P., Cai, S., Gao, Y., Zeng, C., Wan, H., Wang, L., Pan, J., Yu, S., Pan, K., He, J., Lu, X. (2020) Chen, Nat. *Electron.* 3, 563.

[6] Duan, Shengshun., Shi, Qiongfeng., Jun, Wu. (2022). Multimodal Sensors and ML-Based Data Fusion for Advanced Robots, *Advanced Intelligent Systems*, Volume 4 (12), December. p. 220021.3.

[7] Raj, R., Kos, A. (2022). A comprehensive study of mobile robot: history, developments, applications, and future research perspectives. *Applied Sciences,* 12 (14), 6951.

[8] Fottner, J., Clauer, D., Hormes, F., Freitag, M., Beinke, T., Overmeyer, L., Schmidt, T. (2021). Autonomous systems in intralogistics: state of the Art and future research challenges. *Logistics Research*, 14 (1), 1-41.

[9] Fernández Llorca, D., Gómez, E. (2021). Trustworthy autonomous vehicles. Publications Office of the European Union, Luxembourg, *EUR*, 30942.

[10] Ziyuan, Zhong., Hu, Zhisheng., Guo, Shengjian., Zhang, Xinyang., Zhong, Zhenyu., Ray, Baishakhi. (2022). Detecting multi-sensor fusion errors in advanced driver-assistance systems. *Association for Computing Machinery. New York, NY, USA*.

[11] Ogunsina, Morayo., Efunniyi, Christianah Pelumi., Osundare, Olajide Soji., Samuel Olaoluwa Folorunsho and Lucy Anthony Akwawa. (2024). Advanced sensor fusion and localization techniques for autonomous systems: A review and new approaches, *International Journal of Frontline Research in Engineering and Technology*, 2024, 02(01), 051–060.

[12] Jha, S., Rushby, J., Shankar, N. (2020). Model centered assurance for autonomous systems. Paper presented at the Computer Safety, Reliability, and Security: *In*: 39th *International Conference, Safecomp Lisbon, Portugal,* September 16–18, 2020, Proceedings 39.

[13] Vargas, J., Alsweiss, S., Toker, O., Razdan, R., Santos, J. (2021). An overview of autonomous vehicles, sensors, and their vulnerability to weather conditions. *Sensors*, 21 (16), 5397.

[14] Z. Wang, Y. Wu Q. Niu, (2020). Multi-Sensor Fusion in Automated Driving: A Survey, *IEEE Access*, vol. 8, p. 2847-2868.

[15] Khodarahmi, M., Maihami, V. (2023). A review of Kalman filter models. *Archives of Computational Methods in Engineering,* 30 (1), 727-747.

[16] Elfring, J., Torta, E., Van De Molengraft, R. (2021). Particle filters: A hands on tutorial. *Sensors*, 21(2), 438.

[17] Zhang, W. A., Zhang, J., Shi, L., Yang, X. (2024). Gaussian Particle Filtering for Nonlinear Systems with Heavy-Tailed Noises: A Progressive Transform Based Approach. *IEEE Transactions on Cybernetics*.

[18] Mozaffari, S., Al-Jarrah, O. Y., Dianati, M., Jennings, P., Mouzakitis, A. (2020). Deep Learning-Based Vehicle Behavior Prediction for Autonomous Driving Applications: A Review. *IEEE Trans. Intell. Transp. Syst*. 1–15.

[19] Mehra, A., Mandal, M., Narang, P., Chamola, V. (2020). ReViewNet: A Fast and Resource Optimized Network for Enabling Safe Autonomous Driving in Hazy Weather Conditions. *IEEE Trans. Intell. Transp. Syst*. 1–11.

[20] Gonzalez-de-Santos, P., Fernández, R., Sepúlveda, D., Navas, E., Emmi, L., Armada, M. (2020). Field Robots for Intelligent Farms Inhering Features from Industry. *Agronomy* 10, 1638.

[21] Velasco-Hernandez, G., Yeong, D. J., Barry, J., Walsh, J. (2020). Autonomous Driving Architectures, Perception and Data Fusion: A Review. *In: Proceedings of the 2020 IEEE 16th International Conference on Intelligent Computer Communication and Processing (ICCP), Cluj-Napoca, Romania*, 3–5 September.

[22] Yeong, D. J., Velasco-Hernandez, G., Barry, J., Walsh, J. (2021). Sensor and Sensor Fusion Technology in Autonomous Vehicles: A Review. *Sensors* 21, 2140.

[23] Tang, X., Li, B., Du, H. (2023). A Study on Dynamic Motion Planning for Autonomous Vehicles Based on Nonlinear Vehicle Model. *Sensors* 23, 443.

[24] Papaioannou, G., Htike, Z., Lin, C., Siampis, E., Longo, S., Velenis, E. (2022). Multi-Criteria Evaluation for Sorting Motion Planner Alternatives. *Sensors* 22, 5177.

[25] Liao, P., Ning, D., Wang, T., Du, H. (2022). A Driving-Adapt Strategy for the Electric Vehicle with Magneto-Rheological Fluid Transmission Considering the Powertrain Characteristics. *Sensors* 22, 9619.

[26] Zhang, J., Fan, Q., Wang, M., Zhang, B., Chen, Y. (2022). Robust Speed Tracking Control for Future Electric Vehicles under Network-Induced Delay and Road Slope Variation. *Sensors*, 22, 1787.

[27] Yoon, J. Y., Jeong, J., Sung, W. (2022). Design and Implementation of HD Mapping, Vehicle Control, and V2I Communication for Robo-Taxi Services. *Sensors* 22, 7049.

[28] Li, B., Wang, Y., Papaioannou, G., Du, H. (2015). Sensor Fusion and Advanced Controller for Connected and Automated Vehicles. *Sensors* 2023, 23.

[29] Chen, Hongyue., Chen, Hongyan., Xu, Yajun., Zhang, Desheng., Ying Ma, Jun Mao. (2022). Research on attitude monitoring method of advanced hydraulic support based on multi-sensor fusion, *Measurement*, Volume 187,110341.

[30] Xi, Zheng., P., Kolar, S., Bangay, L. (2018). Pan Object localisation through clustering unreliable ultrasonic

range sensors, *Int. J. Sensor Networks*, 27 (4).

[31] Shen, M., Wang, Y., Jiang, Y., et al., (2020). A New Positioning Method Based on Multiple Ultrasonic Sensors for Autonomous Mobile Robot, *Sensors* (Basel, Switzerland) 20(1).